DOI: 10.1002/ejic.200600305

Genotoxic Potential of *N*-(Benzothiazolyl)sulfonamide Copper(II) Complexes on Yeast Cells Transformed with YEGFP Expression Constructs Containing the RAD54 or RNR2 Promoter

Marta González-Álvarez,[a] Gloria Alzuet,[a] Lucas del Castillo,[b] Joaquín Borrás,*[a] and Malva Liu-González[c]

Keywords: Copper complexes / DNA damage / Genotoxicity / yEGFP expression

Four ternary complexes $[Cu(L)_2(phen)]$ where L is an *N*-(benzothiazol-2-yl)sulfonamide derivative have been prepared and their ability to cleave DNA has been studied. The complexes were structurally characterized with the aid of single-crystal X-ray crystallography. Whereas the molecular structure of the $[Cu(L1)_2(phen)]$ (**1**) [HL1 = *N*-(6-chlorobenzothiazol-2-yl)benzenesulfonamide] and $[Cu(L3)_2(phen)]$ (**3**) [HL3 = *N*-(benzothiazol-2-yl)benzenesulfonamide] complexes can best be described as having a distorted square-planar geometry, that of the $[Cu(L4)_2(phen)]$ (**4**) [HL4 = *N*-(benzothiazol-2-yl)toluenesulfonamide] complex shows a strictly square-planar geometry. The $[Cu(L2)_2(phen)MeOH]$ (**2**) [HL2 = *N*-(6-chlorobenzothiazol-2-yl)toluenesulfonamide] complex displays an axially elongated square-pyramidal coordination geometry in which the phen ligand binds at the basal plane. Viscosity and fluorescence measurements indicated that $[Cu(L4)_2(phen)]$ (**4**) has a propensity for binding calf thymus DNA. The four complexes were found to be efficient chemical nucleases, with ascorbate/H_2O_2 activation giving rise to hydroxyl and superoxide radicals as active cleaving species. The nuclease activity of **4** is not only the highest of the four complexes, but also much higher than that of the copper–phenanthroline complex. The ability of the complexes to cleave DNA within cells has been tested by monitoring the expression of the yEGFP gene containing reporter plasmid. The significant induction of fluorescence by complex **4** indicates that it is able to cleave DNA inside the cell.

Introduction

The mechanism of metal carcinogenesis has been widely studied since a number of metals are known to have carcinogenic potential. In 1986, for example, Kawanishi et al.[1] proposed the hypothesis that metal carcinogenesis involves the generation of endogenous reactive oxygen species (ROS). These same researchers subsequently reported that various carcinogenic metal compounds are capable of causing oxidative DNA damage in the presence of H_2O_2.[2–5] Indeed, metals are considered to act not only as carcinogens, but also as cocarcinogens that activate carcinogenic chemicals, since a large number of weak, nonmutagenic carcinogens have been found to act through metal-mediated oxidative DNA damage. Endogenous metals ions such as copper and iron seem to play a particularly important role in ROS generation from various carcinogens, which in turn leads to DNA damage. It has been shown, for example, that in phosphate buffer Cu^{II}/H_2O_2 induces DNA damage at the thymine and guanine positions by generating ROS.[6] Moreover, copper has a dual role in oxidative DNA damage: it generates ROS through autoxidation of carcinogens and also activates H_2O_2 to form a reactive Cu^{I}–hydroperoxo complex.

In recent years the interaction of transition metal complexes with nucleic acids has attracted attention because of their relevance in the development of new reagents for biotechnology and medical research. Interest in the rational design of novel transition metal complexes that bind and cleave duplex DNA with high sequence or structure selectivity has been especially keen. Indeed, there is already a considerable amount of literature that deals with the practical use of transition metal complexes as chemical nucleases. The redox activity of copper complexes of 1,10-phenanthroline as artificial nucleases, for instance, is well known.[7,8] Meunier et al.[9] even developed the Clip-Phen series containing two phen moieties linked through tethers in order to favor the stoichiometry of two phen units per copper. These authors showed that the DNA cleavage activity of copper Clip-Phen complexes increased dramatically in relation to that of the phen parent compound. They then went on to determine the cytostatic activity of these

[a] Departament de Química Inorgànica, Facultat de Farmàcia, Universitat de València,
Avda. Vicente Andrés Estellés s/n, 46100 Burjassot, Spain
Fax: +34-963544960
E-mail: Joaquin.Borras@uv.es
[b] Departament de Microbiologia i Ecologia, Facultat de Farmàcia, Universitat de València,
Avda. Vicente Andrés Estellés s/n, 46100 Burjassot, Spain
[c] SCSIE, RX. Universitat de València,
Dr. Moliner 50, 46100 Burjassot, Spain

complexes.[10] Our group has previously reported[11] several copper ternary complexes of *N*-substituted sulfonamides and phen with the ability to damage DNA in the presence of various reducing agents.

A great number of chemical substances are known to possess in vitro biocatalytic activity, emulating different enzymatic processes. Among these chemicals, copper-coordinated compounds have shown superoxide dismutase and/or DNAsa activities, depending on the type of ligand present. However, in vitro activity occurs under conditions that are usually not equivalent to the physiological environment in the cell. This is an important consideration in evaluating research in this field, as, in order to have any effect, the chemical product in question needs to penetrate within the cell itself. Once the substance is in the cytoplasm, the different mechanisms of cell detoxification can reduce or even prevent its activity, either through degradation or extrusion out of the cell or to intracellular compartments.

In the past, yeast has been used as a model for understanding physiological processes in superior eukaryotes and it is still considered to be an ideal organism for in vivo studies on the activity of biological compounds. Our group has used an *S. cerevisiae* strain deficient in superoxide dismutase for in vivo evaluation of the SOD-like activity of various copper complexes.[12,13] Induction of different yeast genes in response to exposure to DNA-damaging agents represents an important and promising approach for developing genotoxicity tests. Induction of RAD54 and RNR2, two promoters that control the expression of damage-inducible genes, has already been used successfully to evaluate DNA damage.[14–17] We have gone one step further and developed reporter plasmids that express the green fluorescent protein yEGFP gene.[18] The expression of this gene in cells containing the reporter plasmid in response to the exposure to DNA-damaging agents is thus monitored by noting the presence of its characteristic green fluorescence.

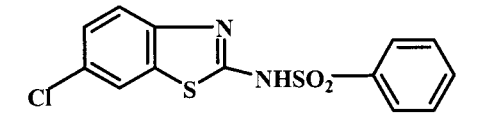

HL1

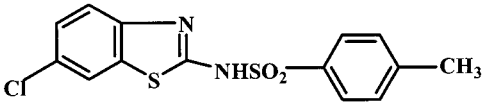

HL2

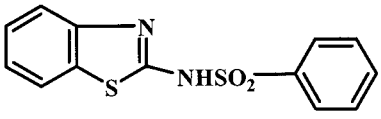

HL3

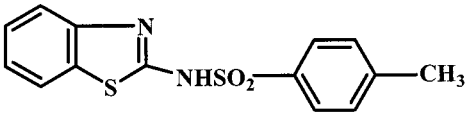

HL4

Scheme 1. *N*-(Benzothiazolyl)sulfonamide ligands.

In this paper we describe the synthesis, characterization, and biological activity assays of four copper ternary complexes with *N*-substituted sulfonamides and *o*-phenanthroline. The sulfonamide ligands selected for this study (Scheme 1) possess two main features that facilitate the synthesis of copper(II) complexes with nuclease activity; both a benzothiazole ring and an aromatic ring (benzene or toluene) able to intercalate between the DNA bases, as well as a sulfonamido group that can interact with DNA through hydrogen bonds. In addition, the benzenesulfonamido group has been suggested to be a functional element that facilitates various biological activities such as the inhibition of tumor cell growth.[19] The biological activity studies include evaluations of DNA binding ability, nuclease activity, and the ability to damage DNA in yeast cells transformed with yEGFP expression constructs containing either the RAD54 or the RNR2 promoter.

Results and Discussion

Spectroscopic and Structural Aspects

Ternary copper(II) complexes $[Cu(L)_2phen]$ (L = L1, L2, L3, and L4) were prepared and characterized with the aid of analytical, spectroscopic, and X-ray diffraction data.

All the complexes had the same infrared spectrum pattern, and the most significant feature was a shift of the characteristic band of the benzothiazole ring from 1550 cm^{-1} in the free ligands to 1460 cm^{-1} in the complexes. As for the sulfonamidato group, the bands assigned to $\nu(SO_2)_{as}$ and $\nu(SO_2)_s$ are shifted to slightly lower frequencies while the ν(S–N) vibration appears at slightly higher frequencies than those of the uncoordinated ligands. In general, the IR spectra are similar to those observed for other copper *N*-sulfonamide derivatives[20,21] with the modifications noted above being mainly because of the ligand deprotonation at the sulfonamide group.

The diffuse reflectance spectra of complexes **1**, **3**, and **4** exhibit a d–d shoulder in the range of 652 to 671 nm while that of complex **2** shows two well-defined d–d bands at 543 and 702 nm. The room temperature magnetic moments of complexes **1** (μ_{eff} = 1.73 BM), **2** (μ_{eff} = 1.75 BM), **3** (μ_{eff} = 1.82 BM), and **4** (μ_{eff} = 1.77 BM) are consistent with the presence of a single unpaired electron. The EPR spectra of the complexes are axial with $g_{\|}$ ranging from 2.22 to 2.30 and $g_{\perp}$ around 2.05.

The complexes have been structurally characterized with the aid of single-crystal X-ray diffraction techniques. ORTEP drawings of the complexes, including the atomic numbering schemes, are shown in Figure 1, Figure 2, Figure 3, and Figure 4. Selected bond lengths and angles are listed in Table 1.

The crystal structures of compounds **1**, **3**, and **4** consist of a discrete monomeric copper(II) species surrounded by

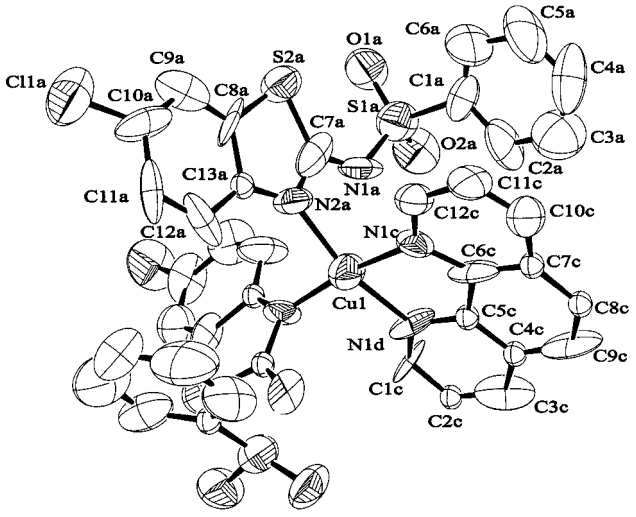

Figure 1. ORTEP drawing of the $[Cu(L1)_2(phen)]$ (**1**) complex.

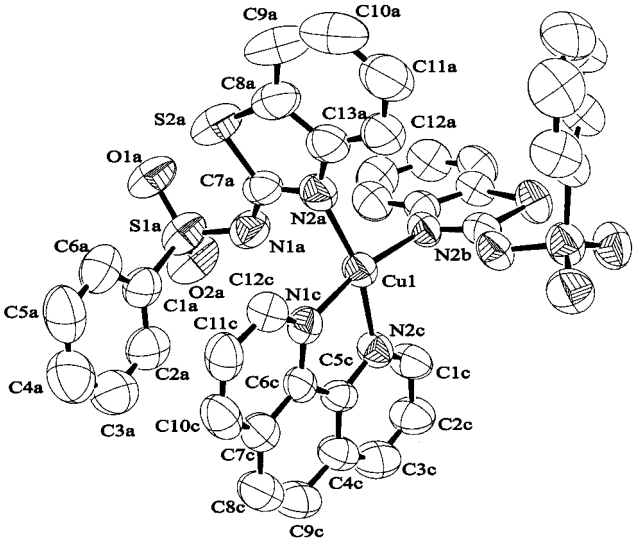

Figure 3. ORTEP drawing of the $[Cu(L3)_2(phen)]$ (**3**) complex.

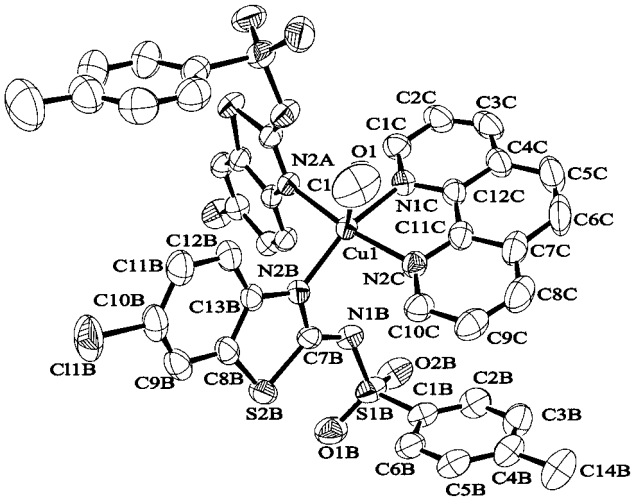

Figure 2. ORTEP drawing of the $[Cu(L2)_2(phen)MeOH]$ (**2**) complex.

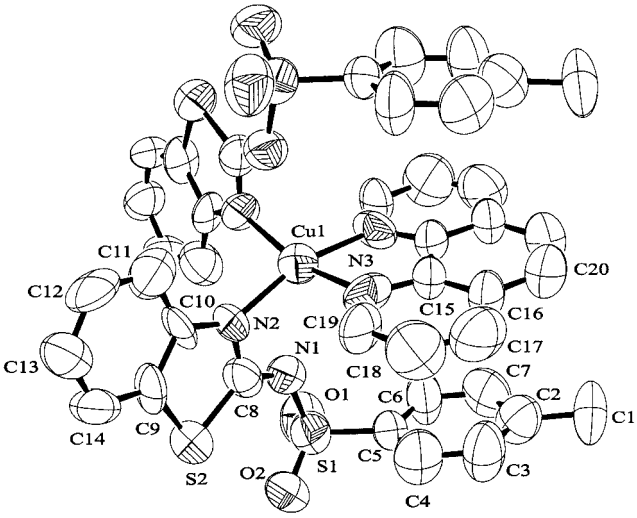

Figure 4. ORTEP drawing of the $[Cu(L4)_2(phen)]$ (**4**) complex.

Table 1. Selected bond lengths [Å] and angles [°] for $[Cu(L1)_2(phen)]$ (**1**), $[Cu(L2)_2(phen)MeOH]$ (**2**), $[Cu(L3)_2(phen)]$ (**3**), and $[Cu(L4)_2(phen)]$ (**4**).

$[Cu(L1)_2(phen)]$		$[Cu(L2)_2(phen)MeOH]$		$[Cu(L3)_2(phen)]$		$[Cu(L4)_2(phen)]$	
Cu(1)–N(2A)	1.989(18)	Cu(1)–N(2B)	1.983(2)	Cu(1)–N(2B)	1.949(4)	Cu(1)–N(2)#1	1.954(15)
Cu(1)–N(2B)	1.989(16)	Cu(1)–N(2A)	2.018(2)	Cu(1)–N(2A)	1.964(4)	Cu(1)–N(2)	1.954(15)
Cu(1)–N(1C)	2.027(12)	Cu(1)–N(1C)	2.020(2)	Cu(1)–N(2C)	2.006(4)	Cu(1)–N(3)	1.989(14)
Cu(1)–N(1D)	1.957(12)	Cu(1)–N(2C)	2.036(2)	Cu(1)–N(1C)	2.013(4)	Cu(1)–N(3)#1	1.989(13)
		Cu(1)–O(1)	2.353(3)				
N(1D)–Cu(1)–N(2B)	96.9(7)	N(2B)–Cu(1)–N(2A)	94.32(9)	N(2B)–Cu(1)–N(2A)	96.93(15)	N(2)#1–Cu(1)–N(2)	94.2(6)
N(1D)–Cu(1)–N(2A)	165.7(9)	N(2B)–Cu(1)–N(1C)	159.55(10)	N(2B)–Cu(1)–N(2C)	92.69(16)	N(2)#1–Cu(1)–N(3)	162.7(7)
N(2B)–Cu(1)–N(2A)	92.6(6)	N(2A)–Cu(1)–N(1C)	91.05(10)	N(2A)–Cu(1)–N(2C)	162.05(19)	N(2)–Cu(1)–N(3)	95.8(10)
N(1D)–Cu(1)–N(1C)	79.9(8)	N(2B)–Cu(1)–N(2C)	93.98(10)	N(2B)–Cu(1)–N(1C)	167.69(17)	N(3)–Cu(1)–N(3)#1	78.(2)
N(2B)–Cu(1)–N(1C)	167.8(8)	N(2A)–Cu(1)–N(2C)	171.67(10)	N(2A)–Cu(1)–N(1C)	92.05(16)	N(1)–Cu(1)–N(2)	58.57(3)
N(2A)–Cu(1)–N(1C)	92.9(7)	N(1C)–Cu(1)–N(2C)	81.35(10)	N(2C)–Cu(1)–N(1C)	80.98(18)	N(1)–Cu(1)–N(3)	91.39(3)
		N(2B)–Cu(1)–O(1)	107.03(11)			N(1)–Cu(1)–N(1)#1	159.03(5)
		N(2A)–Cu(1)–O(1)	98.82(9)			N(1)–Cu(1)–N(2)#1	105.88(3)
		N(1C)–Cu(1)–O(1)	91.57(11)			N(1)–Cu(1)–N(3)#1	104.96(2)
		N(2C)–Cu(1)–O(1)	78.09(9)				

four N atoms belonging to a phenanthroline molecule and two deprotonated *N*-sulfonamide ligands in a distorted square-planar geometry. In complexes **1** and **3** the tetrahedrality value of 15.51° and 18.79°, respectively, indicates that the copper ion adopts a distorted square-planar geometry.[22] The metal ion in complex **4** is located at an inversion symmetry center, hence its coordination polyhedron is strictly square planar. The Cu–N bond lengths lie in the range 1.949(4) to 2.027(12) Å, which are normal lengths for Cu–Nphen and Cu–N-benzothiazole coordination bonds.[11,13,23]

The copper(II) ion in complex **2** is five-coordinate with a distorted square-pyramidal geometry. The basal plane is defined by the benzothiazole N atoms of two deprotonated sulfonamide ligands and the two N atoms of a phenanthroline molecule. The Cu–N bond lengths are similar to those found in complexes **1**, **3**, and **4**. The oxygen atom of a coordinated methanol molecule occupies the axial position with a bond length of 2.353 Å. The changes in bond length are described by tetragonality (T^5); in this case, the tetragonality value of 0.85 fits into the range expected for square-pyramidal complexes with mixed nitrogen-oxygen ligands.[24] The in-plane angular distortion described by the ratio τ represents the percentage of trigonal distortion in a square-pyramidal geometry.[25] The τ value of 0.20 found here thus indicates the presence of a slight distortion.

The coordination mode of the sulfonamide as a monodentate ligand that binds through the benzothiazole N atom in complexes **1**, **2**, **3**, and **4** is the same as that usually found in other Cu^{II} complexes with *N*-substituted sulfonamide analogs.[12,13,23]

DNA Binding Properties

The mode of and propensity for binding of the complexes to calf thymus DNA (CT-DNA) has been studied with the aid of different techniques.

Viscosity Measurements

Viscosity measurements were carried out on CT-DNA by varying the concentration of the complexes. Hydrodynamic measurements that are sensitive to length changes are regarded as the least ambiguous and the most critical tests of binding in solution. One classic intercalation model results in the lengthening of the DNA helix as the base pairs are separated to accommodate the binding ligand, thus leading to the increase of DNA viscosity. In contrast, complexes that bind exclusively in DNA grooves by means of partial and/or nonclassic intercalation under the same conditions typically cause either a less pronounced (positive or negative) or no change in DNA solution viscosity.[26] The results obtained with our compounds reveal that while complex **4** (Figure 5) interacts with DNA in a classic intercalative mode, the presence of complexes **1**, **2**, or **3** (data not shown) has no effect on the relative viscosity of CT-DNA. This indicates that the interaction of these complexes follows the general pattern of other complexes that bind in DNA grooves by either a partial or nonclassic intercalation.

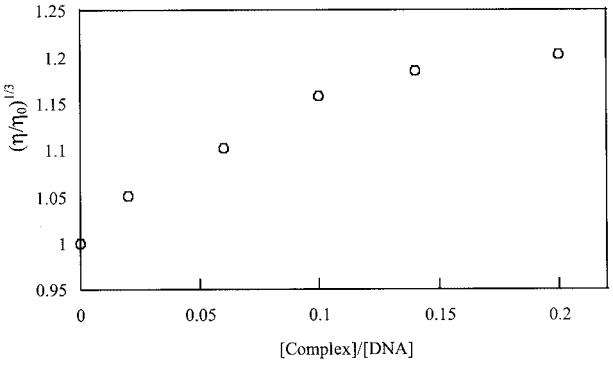

Figure 5. Effect of increasing amounts of the $[Cu(L4)_2(phen)]$ (**4**) complex on the relative viscosity of CT-DNA.

The different behavior exhibited by complex **4** may be attributable to its strictly square-planar geometry; in the other complexes, the distortion of the coordination polyhedron may prevent the intercalation between the bases of the DNA.

Effect of the Complexes on the Emission Spectra of the DNA-EB System

To corroborate the findings from the viscometry results on the mode of DNA interaction, we carried out competitive ethidium bromide (EB) binding studies. Since EB shows a reduced emission intensity in buffers because of the quenching by the solvent molecules and a significantly enhanced intensity when bound to DNA, the emission intensity of this compound is often used as a spectroscopic probe.[27] Binding of the complexes to DNA decreases the emission intensity of EB and the extent of the emission intensity reduction actually gives a measure of the DNA binding propensity of the complexes in question. The results in Figure 6 (a) show that the fluorescence intensity of CT-DNA–EB decreases remarkably with the addition of complex **4**, which indicates that the complex binds to DNA, replacing the EB from the CT-DNA. Such a result is common in intercalative DNA interactions and is consistent with the results obtained from the viscosity measurements.

The fluorescence quenching of EB bound to DNA by complex **4** is in agreement with the classic linear Stern–Volmer equation[27]

$$I_{F0}/I_F = 1 + k_q[Q],$$

where I_{F0} is the emission intensity in the absence of quencher, I_F is the emission intensity in the presence of quencher, k_q is the quenching constant, and $[Q]$ is the quencher concentration. This concordance can be observed by comparing the fluorescence quenching curve of I_{F0}/I_F to the concentration of complex **4** (Figure 6, b). It may thus be concluded that complex **4** binds to DNA mainly by means of intercalation. The value of K_{app} is 1.72×10^6 M^{-1}, which corresponds to the copper(II) complex concentration [Q] = 58.1 μM that causes a 50% quenching of the initial EB fluorescence. This finding suggests that the interaction of **4** with DNA is quite strong.

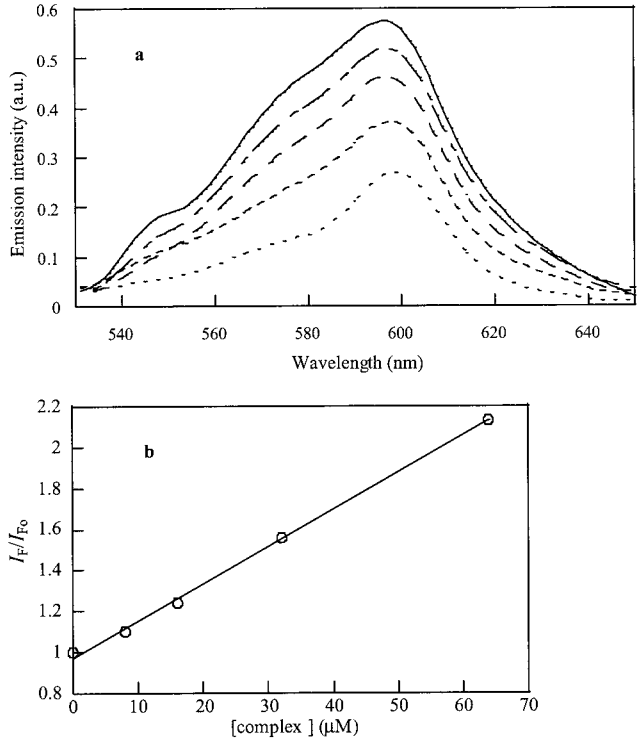

Figure 6. (a) Emission spectra of the DNA–EB system (100 μM CT-DNA base pairs and 10 μM ethidium bromide) λ_{ex} = 500.0 nm λ_{em} = 530–650 nm, in the absence (continuous line) and in the presence (discontinuous lines) of increasing amounts of complex **4** (0–64 μM). (b) Emission quenching of DNA–EB system upon addition of [Cu(L4)$_2$(phen)] (**4**).

The presence of complexes **1**, **2**, or **3** (data not shown) has no effect on the emission spectra of the DNA–EB system under the same conditions.

Thermal Denaturation Results

The binding of complexes **1**–**4** to CT-DNA was then studied from the thermal denaturation profile of DNA. While complexes **1** and **2** produced no increase in the melting temperature (T_m) upon their addition to DNA (CT-DNA T_m = 57 °C), complexes **3** and **4** increased the T_m to 75 and 71 °C, respectively. These results suggest a groove binding for complexes **1** and **2** and intercalation for complexes **3** and **4**, thereby explaining the resulting increased duplex stabilization.[28]

The behavior of complex **3** is noteworthy, especially since the thermal denaturation experiments indicate that this compound can intercalate with DNA while fluorescence and viscosity results do not agree with this result. One possible explanation for the duplex stabilization that is effected by complex **3** is that specific hydrogen-bonding interactions are present between the *N*-(benzothiazolyl)sulfonamide ligands and the bases or phosphate backbone of the DNA. Another possibility is that deformations in the double-helix structure that occur upon binding of the complexes result in additional interstrand interactions.[29]

pUC18 Cleavage

We then went on to study the activity of the complexes as chemical nucleases using supercoiled (SC) pUC18 DNA in cacodylate buffer (pH = 6.0) with ascorbate/H_2O_2 activation. The efficiency of the complexes has been compared with that of both copper salt and the bis(*o*-phenanthroline)-copper complex under the same conditions.

The results shown in Figure 7 indicate that the DNA cleavage activity order is **4** > **2** > **1** > **3**. The results also reveal that the DNA scission mediated by the compounds depends on complex concentration, with the cleavage being more efficient at higher concentrations.

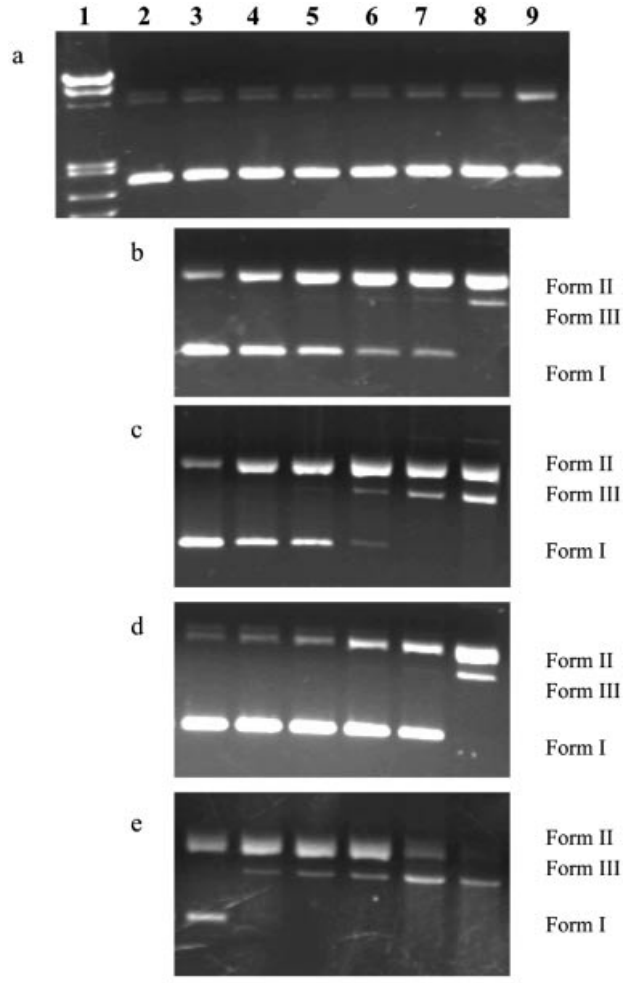

Figure 7. Agarose gel electrophoresis of pUC18 plasmid DNA treated with copper salt, the complexes, or bis(*o*-phenanthroline)-copper(II). [Ascorbate/H_2O_2]:[tested compound] = 1:1. Incubation time: 30 min (37 °C). (a) $CuSO_4$ (b) [Cu(L1)$_2$(phen)] (**1**) complex, (c) [Cu(L2)$_2$(phen)MeOH] (**2**) complex, (d) [Cu(L3)$_2$(phen)] (**3**) complex, (e) [Cu(L4)$_2$(phen)] (**4**) complex.
Lane 1: DNA/EcoRI + Hind III. Marker, 3; lane 2: supercoiled DNA; lane 3: copper salt (a) or complexes (b–e) 1.5 μM; lane 4: copper salt (a) or complexes (b–e) 3 μM; lane 5: copper salt (a) or complexes (b–e) 4.5 μM; lane 6: copper salt (a) or complexes (b–e) 6 μM; lane 7: copper salt (a) or complexes (b–e) 7.5 μM; lane 8: copper salt (a) or complexes (b–e) 9 μM; lane 9: [Cu(phen)$_2$]$^{2+}$ complex 9 μM.

Complexes **1** and **2** at 3 and 4.5 μM (see parts b and c in Figure 7, lanes 4 and 5) produced supercoiled DNA cleavage, which was transformed into circular DNA (Form II). Linearized DNA was not observed under these conditions. This latter finding suggests that cleavage may occur randomly over the DNA since a significant portion of the plasmid already appears to be converted to Form II without concurrent formation of Form III. For its part, Form III resulted from multiple cleavage of Form II and appeared only when full cleavage of Form I was practically achieved (Figure 7, part b, lane 8 and part c, lane 6).

At low concentrations of complex **3** (1.5, 3, and 4.5 μM, lanes 3, 4, and 5 in Figure 7, d) the plasmid remained supercoiled. In contrast to the reactivity of **1** and **2**, complex **3** was unable to mediate the conversion of supercoiled DNA (Form I) at 3 and 4.5 μM (Figure 7, part d, lanes 4 and 5). Upon increasing the concentration of **3** to 6 and 7.5 μM, the supercoiled DNA was partially transformed into open circular DNA (Figure 7, part d, lanes 6 and 7) whereas at 9 μM, DNA Form I was fully converted into Form II and Form III (Figure 7, part d, lane 8).

Complex **4** was the most reactive of the complexes (Figure 7, e), proving to be a very efficient chemical nuclease. At the very low concentration of 1.5 μM, the compound was capable of mediating the conversion of supercoiled DNA to its open circular form (lane 3 in Figure 7, e). In the concentration range from 3 to 6 μM, complex **4** induced complete degradation of the plasmid to yield the open circular and linear forms (Figure 7, part e, lanes 4–6) while at 7.5 μM, the supercoiled DNA was converted into Form II, Form III and small linear fragments that appeared as a smear on the gel (Figure 7, part e, lane 7). At a concentration of 9 μM, only the linear Form III and small linear fragments were observed (Figure 7, part e, lane 8). These products are inconsistent with a mechanism of concerted cleavage of both strains of the plasmid.

As no cleavage was found for $CuSO_4$ under the same conditions (lanes 3–8 of Figure 7, a), the DNA cleavage activity of the compounds can be ascribed to the cooperative effect between Cu^{II} and its ligands.

Since our compounds contain *o*-phenanthroline as a ligand, we have compared their nucleolytic activity with that of bis(*o*-phenanthroline)copper complex, which is a well-known and very efficient chemical nuclease. A comparison of lane 8 of Figure 7, part b (**1**, 9 μM), part c (**2**, 9 μM), part d (**3**, 9 μM), and part e (**4**, 9 μM) with lane 9 of Figure 7 (a) ($[Cu(phen)_2]^{2+}$, 9 μM) clearly indicates that these complexes present considerably higher nuclease activity than the bis(*o*-phenanthroline)copper complex. Under these conditions, bis(*o*-phenanthroline)copper complex was only able to transform a small quantity of SC DNA into its open circular form while the complexes mediated the full conversion of the plasmid Form I to the Forms II and III, with complex **4** producing small linear fragments. It is thus clear that the presence of an *N*-sulfonamide ligand increases nuclease activity.

The existence of diffusible radical species in the nuclease mechanism can be inferred by monitoring the quenching of DNA cleavage in the presence of alternative H-atom donors, which should scavenge radicals (such as $OH^{\cdot}$) in solution. To this end, we included standard scavengers of reactive oxygen intermediates in the electrophoretic process (Figure 8).

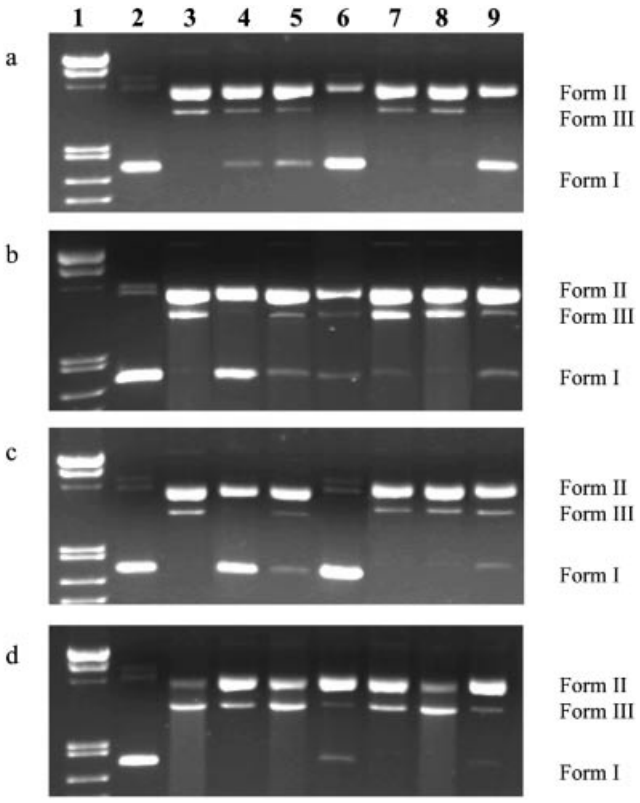

Figure 8. Agarose gel electrophoresis of pUC18 plasmid treated with 9 μM complexes and 9 μM ascorbate/H_2O_2 in the presence of potential inhibitors. Incubation time 30 min (37 °C). (a) $[Cu(L1)_2$-(phen)] (**1**) complex, (b) $[Cu(L2)_2$(phen)MeOH] (**2**) complex, (c) $[Cu(L3)_2$(phen)] (**3**) complex, (d) $[Cu(L4)_2$(phen)] (**4**) complex. Lane 1: DNA/EcoRI + Hind III. Marker, 3; lane 2: supercoiled DNA; lane 3: complex without inhibitors; lane 4: complex + DMSO (1 M); lane 5: complex + *tert*-butyl alcohol (1 M); lane 6: complex + NaN_3(100 mM); lane 7: complex + 2,2,6,6 tetramethyl-4-piperidone (100 mM); lane 8: complex + distamycin (8 μM); lane 9: complex + SOD (15 units).

The presence of the hydroxyl radical scavengers dmso and *tert*-butyl alcohol (lanes 4 and 5 of Figure 8a–d) significantly inhibited the chemical nuclease activity of the complexes. This suggests a cleavage pathway involving the formation of the reactive hydroxyl radical.

Sodium azide (lane 6 of Figure 8, a–d) inhibited DNA cleavage by the compounds to some extent, a finding that points to the participation of $^1O_2$ in the reaction. However, except in the case of **4**, 2,2,6,6-tetramethyl-4-piperidone, another singlet oxygen scavenger, had no observable effect on the cleavage reaction (lanes 7), which clearly contradicts the initial result. This may be resolved by taking into account that since the azide ion can act as a ligand of copper(II), inhibition of the nuclease reaction probably occurs not by radical quenching, but rather by blocking the coordination site on copper that is involved in radical formation. We can

thus conclude that $^1O_2$ is most likely not involved in the reaction.[30]

Lane 9 of Figure 8 (a–d) shows a significant reduction of the DNA cleavage of the complexes in the presence of the SOD enzyme, which indicates that O_2^- is one of the reactive species that actually breaks the DNA.

In the presence of the minor groove binder distamycin (lanes 8), the complexes displayed no apparent inhibition of DNA damage. This suggests that there are no minor binding preferences for the complexes.[31]

The mechanism of the DNA strand scission of bis(*o*-phenanthroline)copper(II) in the presence of reducing agents indicates that upon its reduction, the copper(II) complex binds to DNA, thereby liberating a phenanthroline.[32] Hydrogen peroxide then forms a copper–oxene reactive species that attacks the C1–H of the D-ribose. However, for complexes **1**, **2**, **3**, and **4**, $OH^{\cdot}$ and O_2^- are the active oxygen species involved in the reaction. The involvement of these ROS excludes the formation of a copper–oxene such as that proposed by Sigman for bis(*o*-phenanthroline)copper(II).[32]

Because of the presence of hydroxyl and superoxide radicals and taking into account that the complexes are not able per se to induce any effect on the double stranded DNA, but that the cleavage process can be induced with the addition of activating agents at very low concentrations, we propose that the DNA damage can occur either through a Fenton-type reaction:

$$Cu^{II}(L) + e^- \rightarrow Cu^{I}(L)$$

$$Cu^{I}(L) + H_2O_2 \rightarrow Cu^{II}(L) + OH^- + OH^{\cdot}$$

or a Haber–Weiss reaction:

$$Cu^{II}(L) + e^- \rightarrow Cu^{I}(L)$$

$$Cu^{I}(L) + O_2 \rightarrow Cu^{II}(L) + O_2^-$$

$$O_2^- + H_2O_2 \rightarrow O_2 + OH^- + OH^{\cdot}$$

The proposed mechanism for our compounds is similar to that for the related Cu–*N*-quinolinsulfonamide-*o*-phenanthroline complex.[11]

In summary, the four complexes are very efficient chemical nucleases at low concentrations and in the presence of a low concentration of H_2O_2/ascorbate. In particular, $[Cu(L4)_2(phen)]$ (**4**) is a promising compound with much higher activity than that exhibited by the paradigmatic bis(*o*-phenanthroline)copper(II) complex. The high efficiency of **4** is probably due to the fact that its intercalation binding to DNA permits ROS formation near the deoxyribose moiety. Studies with inhibiting reagents suggest that the cleavage mechanism for these compounds is different from that proposed by Sigman for the bis(*o*-phenanthroline)copper(II) complex.

Genotoxicity Assay in Yeast Cells

Sensitivity of the RAD54-yEGFP and RNR2-yEGFP Reporter System to EMS at Different Incubation Times

Previous studies have shown that the brightness of the fluorescence signal obtained from yeast strains carrying the RAD54-yEGFP promoter-reporter construct on the plasmid correlates with exposure to increasing concentrations of MMS (methyl methane sulfonate).[15] EMS (ethyl methane sulfonate) and MMS are alkylating agents that can act on DNA and lead to damage and mutagenesis. EMS is regularly used as the reference substance for assessing the mutagenic and DNA-damaging potential of chemicals.[14] In order to test the sensitivity of the various transformed

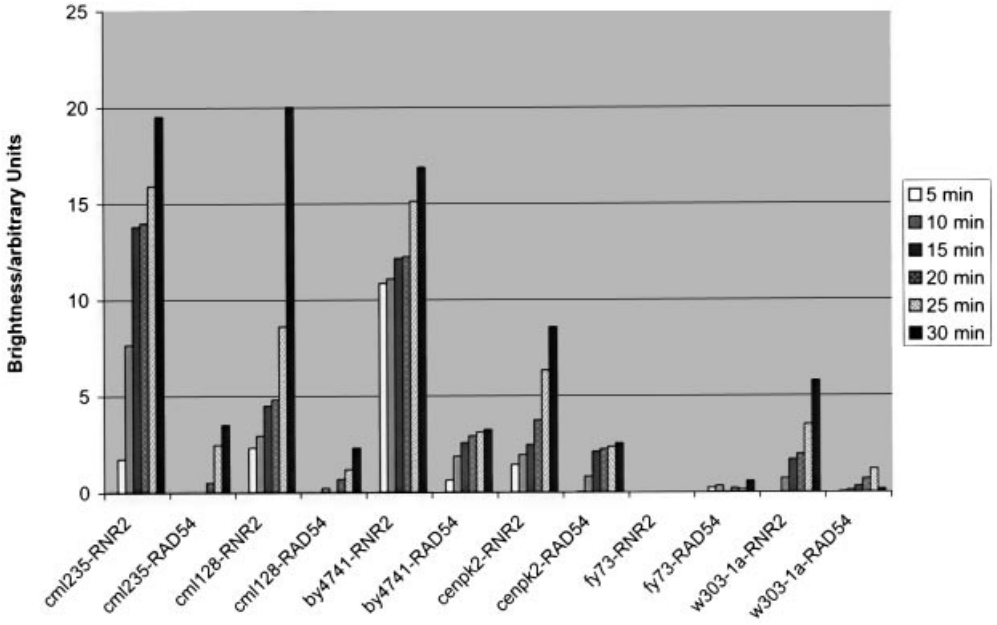

Figure 9. Comparison of EMS-dependent fluorescence in different *Saccharomyces cerevisiae* strains carrying the RAD54-yEGFP or the RNR2-yEGFP constructs. Intensity of the fluorescence signal is dependent on incubation time (0, 5, 10, 15, 20, 25, or 30 min; 0 min is represented as the background). The fluorescence signal displayed has been normalized for cell density.

strains to this paradigmatic mutagenic substance, we have performed fluorescence measurements in response to EMS treatment with yeast cell cultures carrying the RAD54-yEGFP or RNR2-yEGFP constructs. These assays have also been carried out with the aim of selecting the most sensitive transformed stain for subsequent evaluation of the genotoxicity of copper(II) complexes.

The results, shown in Figure 9, demonstrate that after treatment with EMS, only a weak increase in fluorescence is observed with the various RAD54-yEGFP constructions.

As an alternative sensor system, the RAD54 promoter was replaced by the promoter of the RNR2 gene. RNR2, a small subunit of ribonucleoside diphosphate reductase essential for the synthesis of nucleotide precursors, was shown to be induced by MMS treatment.[15] EMS was also able to induce measurable levels of yEGFP fluorescence driven by RNR2, where the fluorescence signal obtained with the RNR2 promoter was stronger than that observed with the RAD54 promoter. This result is consistent with data presented by Jelinsky and Samson[33] and Afanassiev et al.[14] The best results were obtained with the CML128-RNR2 strain, which was consequently chosen to test the ability of the copper compounds to cause DNA damage.

Sensitivity of the CML128-RNR2-yEGFP Reporter System to Copper Compounds at Different Concentrations

The induction of a fluorescence signal driven by promoters that respond to DNA damage in the yeast *S. cerevisiae* provides a system to monitor the activity of substances that possess mutagenic potential at low concentrations. This method not only allows for the recognition of mutagenic agents that are able to produce DNA damage to living systems, but it can also be used to determine the biologically active concentrations of these substances, since the yeast system provides all the typical features of eucaryotic cell architecture and metabolism.

We thus tested the ability of compounds **1**, **2**, **3**, and **4**, previously shown to be strong DNA-cleaving agents, to induce a fluorescence signal in the selected CML128-RNR2-yEGFP system. The response obtained in the presence of $CuCl_2$ or $[Cu(phen)_2]^{2+}$ was studied for comparative purposes while EMS was used as a positive control. Figure 10 shows the intensity of the fluorescence signals induced by EMS, compounds **1**–**4**, and $CuCl_2$ and bis(*o*-phenanthroline)copper(II) over the system after 20 hours of incubation.

As can be seen in Figure 10, complexes **3** and **4** induced fluorescence. In particular, complex **4**, which had been found to be the most efficient chemical nuclease, showed a significant induction of the fluorescence reporter system, which indicates that this compound is able to produce DNA cleavage inside the cell. The signal was much stronger than that of complex **3**. Other substances that have been described in the literature as having induced fluorescence signals over similar systems include cisplatin (a strong DNA cleaving agent), camptothecin (an inhibitor of topoisomerase I), aphidicolin (an inhibitor of DNA polymerases α and δ), and actinomycin D (an intercalator that inhibits mainly transcription, but also replication to some extent).[14]

Complexes **1**, **2**, and bis(*o*-phenanthroline)copper(II), which possesses strong DNA cleaving activity, did not activate the RNR2 promoter-driven yEGFP expression Also, the results show that $CuCl_2$ was unable to induce a fluorescence signal. These negative results observed with complexes **1**, **2**, and bis(*o*-phenanthroline)copper(II), all of which are able to produce pUC18 DNA cleavage, could be because of enzymatic inactivation, lack of cell penetration, detoxification, or other specific properties of the yeast. Some substances known to have mutagenic or DNA-damaging potential, including psoralen, benzpyrene, tetracycline, colchicine, bleomycin, and mitomycin C, are unable to induce activity in similar systems.[14]

Because of the high genotoxic potential of **4**, our next task will be to evaluate the therapeutic use of this compound. With this aim, the potential antitumor activity of **4** will be tested on human tumor cell lines.

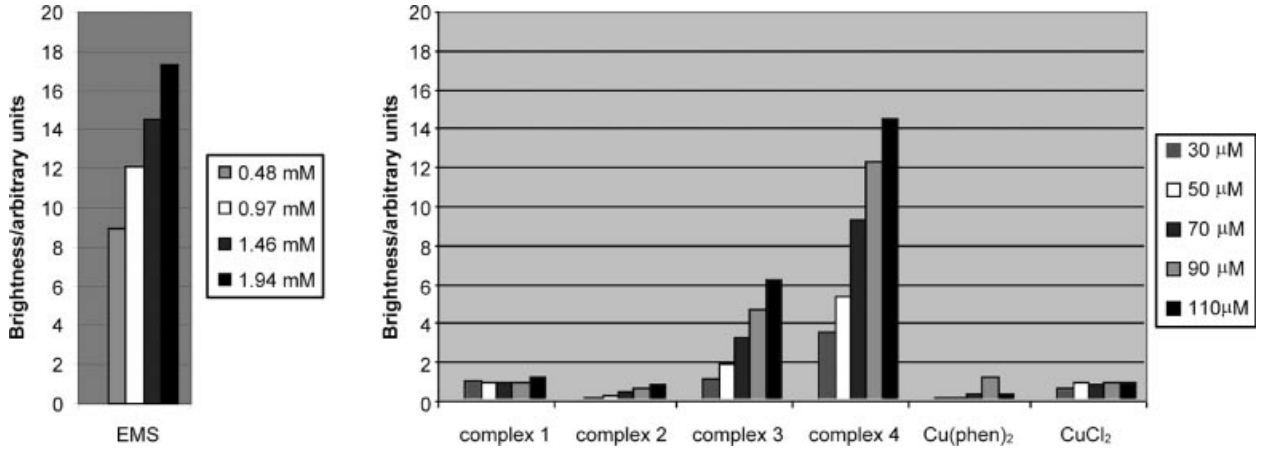

Figure 10. Fluorescence response profiles after treatment of CML128-RNR2-yEGFP with increasing concentrations of EMS, complexes **1**, **2**, **3**, or **4**, $[Cu(phen)_2]^{2+}$, or $CuCl_2$. Diagrams show the dose response of fluorescence after 20 h of incubation (0 M is represented as the background).

Conclusions

Ternary copper(II) complexes with *N*-substituted sulfonamide ligands and *o*-phenanthroline have been prepared and structurally characterized with the aid of X-ray crystallography. The DNA cleavage activities of these complexes have been studied and compared with that of bis(*o*-phenanthroline)copper(II). All the complexes act as efficient chemical nucleases and their activities were found to be higher than that of the paradigmatic bis(*o*-phenanthroline)copper(II) complex. The most active cleaving agent was found to be $[Cu(L4)_2(phen)]$(**4**), which was able to mediate DNA scission at very low concentrations (1.5 μM) in the presence of low concentrations of activating agents. The significant activity of this complex can be ascribed to its efficient binding to DNA, as deduced from viscosity, fluorescence, and thermal denaturation studies. The sensitivity of the CML128-RNR2-yEGFP reporter system to copper compounds was tested to evaluate the genotoxic potential (i.e., the potential to inflict DNA damage) of the compounds at the cellular level. The significant induction of fluorescence by complex **4** indicated a high genotoxic potential for this compound. This fact makes **4** a very promising DNA damaging agent for further studies on human tumor cell lines.

Experimental Section

Materials: Reagents and solvents were commercially available and were used without further purification. pUC18 was purchased from Roche Diagnostics. Calf thymus DNA (CT-DNA) was supplied by Sigma–Aldrich.

Physical Methods: Elemental analyses (C,H,N,S) were performed with a Carlo–Erba AAS instrument. IR spectra (KBr disks) were obtained with a Mattson satellite FT-IR in the range 4000–400 cm^{-1}. Fast atomic bombardment (FAB) mass spectra were obtained with a VG Autospec spectrometer with 3-nitrobenzyl alcohol as the matrix. Diffuse reflectance spectra (nujol mulls) of the complexes were carried out with a Shimadzu UV-2101 PC spectrophotometer. Electronic Paramagnetic Resonance (EPR) spectra were taken at the X-band frequency at room temperature with a Bruker ELEXSYS Spectrometer.

Synthesis of the Ligands

***N*-(Benzothiazol-2-yl)benzenesulfonamide (HL3) and *N*-(Benzothiazol-2-yl)toluenesulfonamide (HL4):** A solution containing 2-aminobenzothiazole (1 g) and benzenesulfonyl chloride (2.5 g) or toluenesulfonyl chloride (2.5 g) in pyridine (6 mL) was heated at reflux for 1 h. The mixture was added to cold water (10 mL) and stirred for several minutes. The resulting solid was recrystallized from ethanol. After several weeks, slow evaporation of the filtrate gave rise to single crystals suitable for X-ray diffraction.

***N*-(Benzothiazol-2-yl)benzenesulfonamide (HL3):** Yield: 1.89 g, 98.9%. $C_{13}H_{10}N_2S_2O_2$ (290.35): calcd. C 53.77; H 3.47; N 9.65; S 20.08; found C 53.88; H 3.26; N 9.69; S 20.05. IR (KBr): $\tilde{\nu}$ = 1561 (thiazole); 1317–1304, 1146 $\nu(SO_2)$; 959 ν(S–N) cm^{-1}. FAB: *m*/*z* = 291 [M^+]. UV: λ_{max} = 309 (π→π*) nm.

***N*-(Benzothiazol-2-yl)toluenesulfonamide (HL4):** Yield: 1.88 g, 93.0%. $C_{14}H_{12}N_2S_2O_2$ (304.38): calcd. C 55.24; H 3.97; N 9.20; S 21.07; found C 55.11; H 3.97; N 9.26; S 21.14. IR (KBr): $\tilde{\nu}$ = 1560 (thiazole); 1314, 1146 $\nu(SO_2)$; 960 ν(S–N) cm^{-1}. FAB: *m*/*z* = 305 [M^+]. UV: λ_{max} = 302 (π→π*) nm.

***N*-(6-Chlorobenzothiazol-2-yl)benzenesulfonamide (HL1) and *N*-(6-Chlorobenzothiazol-2-yl)toluenesulfonamide (HL2):** These compounds were obtained and characterized as previously reported.[23,34]

Synthesis of the Complexes

$[Cu(L1)_2(phen)]$ (1), $[Cu(L2)_2(phen)MeOH]$ (2), $[Cu(L3)_2(phen)]$ (3), and $[Cu(L4)_2(phen)]$(4): Aqueous NaOH (0.5 M, 2 mL) was added to a solution of the ligand (1 mmol) in methanol (40 mL). A suspension of $CuSO_4$ (0.5 mmol) and 1,10-phenanthroline monohydrate (0.5 mmol) in methanol was then added, and the resulting mixture was stirred for ca. 30 min at 40 °C. After cooling, the mixture was filtered to remove the precipitate that formed. Well-shaped crystals of **1**, **3**, and **4** were obtained from the filtrate by slow evaporation at room temperature for several months. Crystals of complex **2** were also formed, but they were not of sufficiently high quality for structural determination. Reaction in methanol by means of slow diffusion afforded good quality crystals of **2** after several days. Crystals of all the complexes were isolated by means of filtration, washed with MeOH, and dried under vacuum.

Complex 1: Yield: 0.142 g, 32%. $C_{38}H_{26}Cl_2CuS_4N_6O_4$: calcd. C 51.09, H 2.93, N 9.41, S 14.36; found C 51.15, H 2.96, N 9.39, S 14.28. IR (KBr): $\tilde{\nu}$ = 1465 (thiazole); 1279, 1129 $\nu(SO_2)$; 961 ν(S–N) cm^{-1}. Solid UV/Vis: λ_{max} = 355 (π→π*), 652 sh (d–d) nm.

Complex 2: Yield: 0.124 g, 26%. $C_{41}H_{32}Cl_2CuS_4N_6O_5$: calcd. C 51.76, H 3.39, N 8.83 S 13.48; found C 51.65, H 3.42, N 8.91 S 13.28. IR(KBr): $\tilde{\nu}$ = 1462 (thiazole); 1295, 1139 $\nu(SO_2)$; 968 ν(S–N) cm^{-1}. Solid UV/Vis: λ_{max} = 338 (π→π*), 543, 702 (d–d) nm.

Complex 3: Yield: 0.152 g, 37%. $C_{38}H_{26}CuS_4N_6O_4$: calcd. C 55.49, H 3.19 N 10.22 S 15.60; found C 55.32, H 3.15 N 10.10 S 15.67. IR (KBr): $\tilde{\nu}$ = 1432 (thiazole); 1276, 1144 $\nu(SO_2)$; 968 ν(S–N) cm^{-1}. Solid UV/Vis: λ_{max} = 371 (π→π*), 671 sh (d–d) nm.

Complex 4: Yield: 0.115 g, 27%. $C_{40}H_{30}CuS_4N_6O_4$: calcd. C 56.49 H 3.56 N 9.88 S 15.08. found C 56.53 H 3.42 N 9.88 S 15.08. IR(KBr): $\tilde{\nu}$ = 1489–1441 (thiazole); 1276, 1134 $\nu(SO_2)$; 967 ν(S–N) cm^{-1}. Solid UV/Vis: λ_{max} = 337 (π→π*), 665 sh (d–d) nm.

X-ray Crystallography: A green crystal measuring 0.04 × 0.04 × 0.08 mm (**1**), a blue crystal measuring 0.2 × 0.08 × 0.24 mm (**2**), a brown crystal measuring 0.04 × 0.1 × 0.2 mm (**3**), and a dark blue crystal measuring 0.14 × 0.12 × 0.08 mm (**4**), and either a triclinic space group $P\bar{1}$ (**1**) or a monoclinic space group *P*21/*c* (**2**, **3**, and **4**) (as determined from systematic absences) were used. Data collection was performed at 293 K with a Nonius Kappa-2000 single crystal diffractometer, with Cu-K_α radiation (λ = 1.54184 Å) for complexes **1**, **3**, and **4** or with a Nonius Kappa CCD single crystal diffractometer with Mo-K_α radiation (λ = 0.71073 Å) for complex **2**. The crystal-detector distance was fixed at 35 mm (**1**, **3**, and **4**) or 32.1 mm (**2**) and a total of 106 (**1**), 228 (**2**), 430 (**3**), and 91 (**4**) images were collected by means of the oscillation method, with a scan angle per frame of 2° (**1**, **3**, and **4**) or 1.7° (**2**) oscillation and 20 s (**1**), 15 s (**2**), 26 s (**3**), and 2 s (**4**) exposure time per image. The data collection was carried out and calculated with the program Collect.[35] Data reduction and cell refinements were performed with the programs HKL Denzo and Scalepack.[36]

Unit cell dimensions were determined from 295 (**1**), 10423 (**2**), 3916 (**3**), and 597 (**4**) reflections between θ = 0.999° and 39.973° (**1**),

0.998° and 28.7° (**2**), 0.999° and 63.691° (**3**), and 0.99° and 36.05° (**4**). Multiple observations were averaged: for complex **1** (R_{merge} = 0.0000) this resulted in 1712 unique reflections of which 1189 were observed with $I > 2\sigma(I)$, for complex **2** (R_{merge} = 0.030) this resulted in 10601 unique reflections of which 6891 were observed with $I > 2\sigma(I)$, for complex **3** (R_{merge} = 0.0000) this resulted in 4086 unique reflections of which 2439 were observed with $I > 2\sigma(I)$, and for complex **4** (R_{merge} = 0.0000) this resulted in 879 unique reflections of which 732 were observed with $I > 2\sigma(I)$. Final mosaicity was 0.35(**1**), 0.43 (**2**), 0.50 (**3**), and 0.509 (**4**). All data completeness was 74.2% (**1**), 98.2% (**2**), 84.0% (**3**), and 95.5% (**4**).

Crystal structures were solved by direct methods, either with the program SIR-97 (**1**, **2**, and **3**) or SHELXS-86 (**4**).[37] Anisotropic least-squares refinements were carried out with SHELXL-97.[38] All non-hydrogen atoms were anisotropically refined while hydrogen atoms were located geometrically. The final cycle of full-matrix least-squares refinement based on 1712 (**1**), 10601 (**2**), 4086 (**3**), and 879 (**4**) reflections and 494 (**1**), 536 (**2**), 561 (**3**), and 284 (**4**) parameters converged to a final value of R_1 [$F^2 > 2\sigma(F^2)$] = 0.052, wR_2 [$F^2 > 2\sigma(F^2)$] = 0.130, R_1 (F^2) = 0.082, wR_2 (F^2) = 0.150 for complex **1**; R_1 [$F^2 > 2\sigma(F^2)$] = 0.046, wR_2 [$F^2 > 2\sigma(F^2)$] = 0.127, R_1 (F^2) = 0.090, wR_2 (F^2) = 0.170 for complex **2**; R_1 [$F^2 > 2\sigma(F^2)$] = 0.044, wR_2 [$F^2 > 2\sigma(F^2)$] = 0.094, R_1 (F^2) = 0.092, wR_2 (F^2) = 0.112 for complex **3**; and R_1 [$F^2 > 2\sigma(F^2)$] = 0.036, wR_2 [$F^2 > 2\sigma(F^2)$] = 0.097, R_1 (F^2) = 0.045, wR_2 (F^2) = 0.105 for complex **4**. Final difference Fourier maps showed no peaks higher than 0.261 e/Å^3 nor deeper than –0.397 e/Å^3 for complex **1**, no peaks higher than 0.678 e/Å^3 to 1.06 Å to H14d nor deeper than 1.5 e/Å^3 to 0.85 Å to Cu for complex **2**, no peaks higher than 0.197 e/Å^3 to 1.14 Å to N1c nor deeper than –0.405 e/Å^3 to 0.98 to Cu1 for complex **3**, and no peaks higher than 0.411 e/Å^3 nor deeper than –0.167 e/Å^3 for complex **4**. Semi-empirical absorption correction was applied using the program XABS2[39] for complex **1**. Geometrical calculations were made with PARST.[40] The crystallographic plots were made with ORTEP.[41] A summary of crystallographic data of the complexes is given in Table 2.

The supplementary crystallographic data for this paper is contained in CCDC-299259, -299260, -299261, and -299262. These data can be obtained free of charge from The Cambridge Crystallographic Data Centre via www.ccdc.cam.ac.uk/data_request/cif.

Metal Complexes–DNA Interactions

Viscosity Measurements: Viscosity experiments were carried out with a Cannon 25 L97 viscosimeter immersed in a Julabo thermostatted water bath maintained at 25.0 ± 0.1 °C. Solutions of the complexes (1–10 μM) in cacodylate buffer (pH = 6.0) were added to a calf thymus DNA (50 μM base pairs) solution in cacodylate buffer. The flow times were measured with a digital stopwatch. The flow measurements were performed in triplicate. Data were presented as $(\eta/\eta_0)^{1/3}$ vs. the ratio of the concentration of complex and DNA, where η is the viscosity of DNA in the presence of the complex and η_0 is the viscosity of DNA alone. Viscosity values were calculated from the observed flow time of a DNA-containing solution corrected from the flow time of buffer alone (t_0), $\eta = t - t_0$.

Fluorescence Quenching of Ethidium Bromide Intercalated to DNA by Interaction of the Copper Complexes with DNA: The fluorescence spectra were recorded with a JASCO FP-6200 spectrofluorimeter at room temperature. The experiments were conducted by adding copper(II) complex solutions at various concentrations (0–64 μM) to samples containing 100 μM calf thymus DNA base pairs and 10 μM ethidium bromide in cacodylate buffer (pH = 6.0). All the samples were excited at 500 nm and emission was recorded at 530–650 nm.

Thermal Denaturation Experiments: DNA-melting experiments were carried out by monitoring the absorbance (260 nm) of CT-DNA (100 μM base pairs) at different temperatures in the absence and presence of the complexes in a 4:1 DNA/complex ratio. Measurements were performed with an Agilent 8453 UV/Vis spectrophotometer equipped with a Peltier temperature controlled sample cell and driver (Agilent 89090A). The solution containing the ternary complex and CT-DNA in phosphate buffer (1 mM phosphate, 2 mM NaCl, pH = 7.2) was continuously stirred and heated with a rate of temperature increase of 1 °C/min. The temperature interval studied ranged from 25 to 90 °C.

pUC18 DNA Cleavage: A typical reaction for complexes was undertaken by mixing a cacodylate buffer (0.1 M, 7 μL, pH 6.0), pUC18 (1 μL, 0.25 μg/μL), a solution of the tested complex (6 μL) at increasing concentrations between 1.5 μM and 9 μM, ascorbate (3 μL), and a H_2O_2 (3 μL) twofold molar excess relative to the concentration of the complex in cacodylate buffer. The mixtures were allowed

Table 2. Crystal data and structure refinement for [Cu(L1)$_2$(phen)] (**1**), [Cu(L2)$_2$(phen)MeOH] (**2**), [Cu(L3)$_2$(phen)] (**3**), and [Cu(L4)$_2$-(phen)] (**4**).

Compound	**1**	**2**	**3**	**4**
Empirical formula	$C_{38}H_{26}Cl_2CuN_6O_4S_4$	$C_{41}H_{32}Cl_2CuN_6O_5S_4$	$C_{38}H_{26}CuN_6O_4S_4$	$C_{20}H_{15}Cu_{0.5}N_3O_2S_2$
Formula mass [g/mol]	893.33	958.41	822.43	425.24
Crystal system	triclinic	monoclinic	monoclinic	monoclinic
Space group	$P\bar{1}$	$P2_1/c$	$P2_1/c$	$P2_1/c$
a [Å]	10.8510(9)	17.4880(2)	11.6840(3)	12.0450(7)
b [Å]	11.4360(7)	11.7090(2)	18.0120(5)	11.3450(6)
c [Å]	15.6000(12)	20.5440(2)	17.2570(3)	17.8480(10)
α [°]	86.714(3)	90	90	90
β [°]	81.697(3)	95.7960(7)	101.2430(11)	126.072(3)
γ [°]	89.291(3)	90	90	90
V [Å^3]	1912.4(2)	4185.23(10)	3562.08(15)	1971.34(19)
Z	2	4	4	4
λ [Å]	1.54184	0.71073	1.54184	1.54184
μ [mm^{-1}]	4.551	0.903	3.485	3.167
$\rho_{calcd.}$ [mg/m^3]	1.551	1.521	1.534	1.433
T [K]	293(2)	293(2)	293(2)	293(2)
R_1	0.0523	0.0458	0.0437	0.0361
wR_2	0.1304	0.1271	0.0941	0.0971

to stand for 30 min at 37 °C. After that, a quench buffer solution (3 μL) consisting of bromophenole blue (0.25%), xylene cyanole (0.25%), and glycerol (30%) were added. The solution was then subjected to electrophoresis on a 0.8% agarose gel in 0.5×TBE buffer (0.045 M Tris, 0.045 M boric acid, and 1 mM EDTA) containing 2 μL/100 mL of a solution of ethidium bromide (10 mg/mL) at 80 V for about 2 h. The gel was photographed on a capturing gel printer plus TDI.

To test for the presence of reactive oxygen species (ROS) generated during strand scission, various reactive oxygen intermediate scavengers were added to the reaction mixtures. The scavengers used were superoxide dismutase (15 units), DMSO (1 M), *tert*-butyl alcohol (1 M), sodium azide (100 mM), and 2,2,6,6-tetramethyl-4-piperidone (100 mM). An assay in the presence of the minor groove binder distamycin (8 μM) was also performed. Samples were treated as described above.

Genotoxicity Assays

Construction of a Plasmid Containing yEGFP Under the Transcriptional Control of the RNR2 or RAD54 Promoter: PCR was used to amplify the RNR2 and RAD54 promoters from genomic *Saccharomyces cerevisiae* DNA with the primers shown in Table 3. pUG35 plasmid was digested with Sal I and Sac I to remove the original promoter of yEGFP. The PCR products were digested with the same restriction enzymes and were ligated into the pUG35 to produce pUG35-RNR2 or pUG35-RAD54. The yeast strains used in this study, listed in Table 4, were grown on a YNB medium (1.68 g of YNB without aa and without salts, 5 g of ammonium sulfate, and 20 g of glucose per liter) with the required amino acids.

Table 3. Primers used in the construction of the RAD54-yRGFD or RNR2-yEGFD promoter-reporter plasmid.

RAD54-3SAL	GGC CGT TCA CCG TCG ACT ATT CC
RAD54-5SAC	AAA ATA TTG AGC TCG AAG ATC TGT CC
RNR2-3SAL	GGA CAA TGC GTC GAC AGC AG
RNR2-5SAC	TAG CCA GAG CTC TGC ATT ACG C

Table 4. Yeast strain used.

Strain	Relevant genotype
BY4741	MATa his3-δ1 leu2-δ0 met15-δ0 ura3-δ0
CML235	MATa his3-δ200 ura3-52 leu3-δ1
W303-1A	MATa ura3-1 ade2-1 leu2-3,112 trp1-1 his3-11,15
CML128	MATa leu2-3,112 ura3-52 trp1-1 his4 can1r
CEN.PK2	MATa/MATα ura3-52/ura3-52 trp1-289/trp1-289 leu2-3,112/leu2-3,112 his3δ1/his3δ1
FY73	MATα his3-Δ200, ura3-52
Transformed reporter strains	
BY4741-RAD54	BY4741 transformed with pUG35-RAD54
CML235-RAD54	CML235 transformed with pUG35-RAD54
W303-1A-RAD54	W303-1A transformed with pUG35-RAD54
CML128-RAD54	CML128 transformed with pUG35-RAD54
CEN.PK2-RAD54	CEN.PK2 transformed with pUG35-RAD54
FY73-RAD54	FY73 transformed with pUG35-RAD54
BY4741-RNR2	BY4741 transformed with pUG35-RNR2
CML235-RNR2	CML235 transformed with pUG35-RNR2
W303-1A-RNR2	W303-1A transformed with pUG35-RNR2
CML128-RNR2	CML128 transformed with pUG35-RNR2
CEN.PK2-RNR2	CEN.PK2 transformed with pUG35-RNR2
FY73-RNR2	FY73 transformed with pUG35-RNR2

Sensitivity of the RAD54-yEGFP and RNR2-yEGFP Reporter Systems to EMS: Liquid YNB (10 mL; 1.68 g of YNB without aa and without salts, 5 g of ammonium sulfate, and 20 g of glucose per liter) with the suitable requirements were inoculated into a fresh sample of the yeast strain to give approximately 1×10^6 cells/mL. The cultures were incubated overnight at 28 °C with vigorous shaking. The cultures were then washed twice in 50 mM potassium phosphate buffer (pH = 7.0) and resuspended in this buffer to a final concentration of 5×10^7 cells/mL. EMS (30 μL) was added to 1 mL of cells and incubated for 30 min at 30 °C. 100 μL samples were obtained at different times (0, 5, 10, 15, 20, 25, and 30 min) during the incubation. The EMS mutagenesis was stopped in each cell suspension by adding an equal volume of a freshly made 10% (w/v) filter-sterilized solution of sodium thiosulfate. The suspensions were then mixed well and centrifuged, after which the cells were collected and washed twice with sterile water. The cells were then inoculated in liquid medium and incubated at 28 °C for 20 h on an orbital shaker. For cell fluorescence measurements, the cell cultures were diluted (1:10 in sterile distilled water) and transferred directly to cuvettes. Samples with cell cultures with no mutagenic agents were taken as blanks. Fluorescence measurements were performed with a Jasco FP-6200 spectrofluorometer. The excitation and emission wavelengths were set to 488 and 511 nm, respectively, with a slit width of 10 nm. Fluorescence values were normalized for the absorption values of each cell. The normalized fluorescence values were then plotted against the substance concentration and incubation time. All calculations and plots were made with MS Excel.

Evaluation of Genotoxicity Produced by the Complexes: Single colonies of the selected transformed yeast strains grown on selective medium were used to inoculate 5 mL of medium and then grown to mid log phase (0.4 AU at 600 nm). The cells were resuspended in fresh medium to a final concentration of 0.1 AU. Solutions of EMS, the copper salt, or the test compounds at increasing concentrations were distributed in parallel. The tubes were incubated at 28 °C for 20 h on an orbital shaker at 120 rpm. Fluorescence measurements were performed as described above except that, in this case, the first measurement was taken at 0 h and repeated at 4, 16, and 20 h of incubation.

Acknowledgments

J. B. and G. A. acknowledge financial support from the Spanish CICYT (CTQ2004-03735). M. G.-A. wishes to thank the city government of Valencia (Spain) for a Carmen and Severo Ochoa postdoctoral fellowship.

[1] S. Kawanishi, Y. Hiraku, M. Murata, S. Oikawa, *J. Biol. Chem.* **1986**, *261*, 5952–5958.
[2] S. Inoue, S. Kawanishi, *Cancer Res.* **1987**, *47*, 6522–6527.
[3] K. Yamamoto, S. Inoue, T. Yoshinaga, S. Kawanishi, *Chem. Res. Toxicol.* **1989**, *2*, 234–239.
[4] S. Kawanishi, S. Inoue, K. Yamamoto, *Carcinogenesis* **1989**, *10*, 2231–2235.
[5] S. Inoue, S. Kawanishi, *Biochem. Biophys. Res. Commun.* **1989**, *159*, 445–451.
[6] K. Yamamoto, S. Kawanishi, *J. Biol. Chem.* **1989**, *264*, 15435–15440.
[7] P. M. Doraiswamy, A. E. Finefrock, *Lancet Neurol.* **2004**, *3*, 431–434.
[8] K. J. Barnham, C. L. Masters, A. I. Bush, *Nat. Rev. Drug Discovery* **2004**, *3*, 205–214.
[9] M. Pitié, C. Boldron, H. Gortnitzka, C. Hemmert, B. Donnadieu, B. Meunier, *Eur. J. Inorg. Chem.* **2003**, 528–540.
[10] M. Pitié, A. Croisy, D. Carrez, C. Boldron, B. Meunier, *ChemBioChem* **2005**, *6*, 686–691.
[11] B. Macías, I. García, M. J. Villa, M. González-Álvarez, J. Borrás, A. Castiñeiras, *J. Inorg. Biochem.* **2003**, *96*, 367–374.

[12] M. González-Álvarez, G. Alzuet, J. Borrás, L. del Castillo Agudo, S. García-Granda, J. M. Montejo-Bernardo, *J. Biol. Inorg. Chem.* **2003**, *8*, 112–120.
[13] M. González-Álvarez, G. Alzuet, J. Borrás, L. del Castillo Agudo, S. García-Granda, J. M. Montejo-Bernardo, *Inorg. Chem.* **2005**, *44*, 9424–9433.
[14] V. Afanassiev, M. Sefton, T. Anantachaiyong, G. Barker, R. Walmsley, S. Wölfl, *Mutat. Res.* **2000**, *464*, 297–308.
[15] N. Billinton, M. G. Barker, C. E. Michel, A. N. Knight, W. D. Heyer, N. J. Goddard, P. R. Fielden, R. M. Walmsley, *Biosens. Bioelectron.* **1998**, *13*, 831–838.
[16] R. M. Walmsley, N. Billinton, W. D. Heyer, *Yeast* **1997**,*13*, 1535–1545.
[17] D. Averbeck, S. Averbeck, *Mutat. Res.* **1994**, *315*, 123–138.
[18] B. P. Cormack, G. Bertram, M. Egerton, N. A. R. Gow, S. Falkow, A. J. P. Brown, *Microbiology* **1997**, *143*, 303–311.
[19] Y.-H. Kim, K.-J. Shin, T. G. Lee, E. Kim, M.-S. Lee, S. H. Ryu, P.-G. Suh, *Biochem. Pharmacol.* **2005**, *69*, 1333–1341.
[20] R. Cejudo-Marín, G. Alzuet, S. Ferrer, J. Borrás, A. Castiñeiras, E. Monzani, L. Casella, *Inorg. Chem.* **2004**, *43*, 6805–6814.
[21] L. Gutiérrez, G. Alzuet, J. A. Real, J. Borrás, A. Castiñeiras, *Eur. J. Inorg. Chem.* **2002**, 2094–2102.
[22] L. P. Battaglia, A. Bonamartini-Corradi, G. Marcotrigiano, L. Menabue, G. C. Pellacani, *Inorg. Chem.* **1979**, *18*, 148–152.
[23] M. González-Álvarez, G. Alzuet, J. Borrás, L. del Castillo Agudo, S. García-Granda, J. M. Montejo-Bernardo, *J. Inorg. Biochem.* **2004**, *98*, 189–198.
[24] B. J. Hathaway, *Comprehensive Coordination Chemistry* (Eds.: R. D. Gillard, J. A. McCleverty), Pergamon, New York, **1987**, ch. 9, 535–591.
[25] W. Addison, T. N. Rao, J. Reedijk, J. van Rijn, G. C. Verschoor, *J. Chem. Soc., Dalton Trans.* **1984**, 1349–1356.
[26] J. Liu, T. Zhang, L. Qu, H. Zhou, Q. Zhang, J. Liangnian, *J. Inorg. Biochem.* **2002**, *91*, 269–276.
[27] Y. B. Zeng, N. Tang, W. S. Liu, N. Tang, *J. Inorg. Biochem.* **2003**, *97*, 258–264.
[28] S. Dhar, M. Nethaji, A. R. Chakravarty, *Inorg. Chem.* **2005**, *44*, 8876–8883.
[29] K.-L. Fu, P. M. Bradley, C. Turro, *Inorg. Chem.* **2003**, *42*, 878–884.
[30] M. González-Álvarez, G. Alzuet, J. Borrás, M. Pitié, B. Meunier, *J. Biol. Inorg. Chem.* **2003**, *8*, 644–652.
[31] N. Jiménez-Garrido, L. Perelló, R. Ortiz, G. Alzuet, M. González-Álvarez, E. Cantón, M. Liu-González, S. García-Granda, M. Pérez-Priede, *J. Inorg. Biochem.* **2005**, *99*, 677–689.
[32] D. S. Sigman, R. Landgraf, D. Perrin, M. L. Pearson, *Metal Ions in Biological Systems 33* (Eds.: A. Sigel, H. Sigel), Marcel Dekker Inc., New York, **1996**, pp. 485–523.
[33] S. A. Jelisnky, L. D. Samson, *Proc. Natl. Acad. Sci. USA*. **1999**, *96*, 1486–1491.
[34] M. González-Álvarez, G. Alzuet, J. Borrás, B. Macías, J. M. Montejo-Bernardo, S. García-Granda, *Z. Anorg. Allg. Chem.* **2003**, *629*, 239–243.
[35] COLLECT, B. V. Nonius, **1997–2000**.
[36] Z. Otwinowski, W. Minor, "Processing of X-ray Diffraction Data Collected in Oscillation Mode" in *Methods in Enzymology*, vol. 276 (Macromolecular Crystallography, Part A), Carter and Sweet, Academic Press, New York, **1997**, pp. 307–326.
[37] G. M. Sheldrick, SHELX-86, *Program for Crystal Structure Solution*, University of Göttingen, Germany, **1986**.
[38] G. M. Sheldrick, SHELX97, *Programs for Crystal Structure Analysis* (Release 97-2), University of Göttingen, Germany, **1997**.
[39] *XABS2*: S. Parkin, B. Moezzi, H. Hope, *J. Appl. Crystallogr.* **1995**, *28*, 53–56.
[40] *PARST*: a) M. Nardelli, *Comput. Chem.* **1983**, *7*, 95–97; b) M. Nardelli, *J. Appl. Crystallogr.* **1995**, *28*, 659.
[41] *ORTEP3 for Windows*: L. J. Farrugia, *J. Appl. Crystallogr.* **1997**, *30*, 565.

Received: April 5, 2006
Published Online: July 25, 2006

